Determination of the analytical and the nonanalytical part of the exchange interaction of InP and GaAs from polariton spectra in intermediate magnetic fields

W. Ekardt
Fritz-Haber-Institut der Max-Planck-Gesellschaft, Faradayweg 4-6, D-1000 Berlin 33, West Germany

K. Lösch*
Physikalisches Institut (Teil 4) der Universitat Stuttgart, Pfaffenwaldring 57, D-7000 Stuttgart 80, West Germany

D. Bimberg†
Hochfeld-Magnetlabor des Max-Planck-Institut für Festkörperforschung, 166X, F-38042 Grenoble, France

(Received 14 February 1979)

The isotropic analytical exchange interaction Δ_a of GaAs and InP is determined to be 0.02 ± 0.01 and 0.04 ± 0.015 meV, respectively, for the two materials from a comparison of theoretically generated and experimentally determined transverse exciton energies and oscillator strengths in magnetic fields up to 20 T. The calculation of the theoretical spectra is based on a recent intermediate-field theory including the analytical and nonanalytical part of the exchange interaction. The experimental values are determined from a two-oscillator line-shape analysis of σ^-,- σ^+-, and π-polarized magnetoreflection spectra. A newly developed model describing the exciton-free surface layer of a semiconductor by an exponentially decreasing damping of the exciton contribution to the dielectric constant is shown to improve strongly the quality of the line-shape fit. This improvement is achieved without increasing the number of fitting parameters as compared to the older model using a layer of finite thickness with infinite damping. From a similar comparison of theoretical and experimental values of the energies and oscillator strengths of longitudinal-transverse mixed-mode exciton spectra in magnetic fields which are found for the σ polarization in Voigt configuration ($\vec{k} \perp \vec{H}$) the size of the nonanalytical exchange interaction Δ_{LT} in GaAs is determined to be 0.08 ± 0.02 meV. For InP an upper limit of $\Delta_{LT} \leq 0.1$ meV is derived.

I. INTRODUCTION

The theoretical understanding and the experimental characterization of the excitonic polariton in cubic direct-gap semiconductors including the effects of external magnetic fields has progressed rapidly during the last years. This was partly stimulated by the success of Baldereschi and Lipari[1] (BL) in solving the Schrödinger equation of the free exciton *including* the complex sixfold degenerate valence band, in contrast to the earlier simplifying isotropic two-band models.[2] High-resolution magnetoreflectance investigations of a series of semiconductors gave direct evidence for effects due to the degenerate band structure revealing, e.g., polarization- (and therefore M_J) dependent diamagnetic effects.[3] These and other experiments showed simultaneously that a correct understanding can only be reached if the exchange interaction and the interaction of the exciton with the radiation field (polariton picture) is included in the description of both the experiment and theory and if an exciton-free layer at the surface of the crystal is assumed.[4–8]

The low-magnetic-field theories of Cho *et al.*[9] and Swierkowski[10] account for the band-structure and short-range exchange effects. Unfortunately, there are only few experimental results available to be compared directly with these perturbation theories which are limited to rather low magnetic fields $H \leq 0.3\gamma$, where $\gamma = 0.5\hbar\omega_c/R$ is a relative measure of the magnetic field, with $\omega_c = e\hbar/m^*c$ and $R = (13.6 \text{ eV}) m^*/m_0\epsilon^2$.

The adiabatic-high-field theory of Altarelli and Lipari[11] (AL) was recently[6,7] successfully applied to analyze the field dependence of the energies of the six σ^+-, σ^--, and π-polarized exciton ground states of GaAs and InP. The Luttinger parameters γ_1, γ_2, γ_3, and κ were derived from this analysis, which were subsequently found to well describe the acceptor spectra.[12] However, the interpretation of the strong dependence of the σ spectra on the direction of the wave vector $\vec{k}$ of the light relative to the magnetic field axis $\vec{H}$ observed for both materials is beyond the scope of the theory of AL at its present state.

On the other hand, one of us (W. E.) developed a rather general theory for intermediate magnetic fields,[13–15] including the analytical and nonanalytical parts of the exchange interaction, and covering very well a range of fields $1.0 \leq \gamma \leq 5$ for which precise experimental data are available. The band-structure parameters employed to give a good description of

the experimental field dependence of the energies in the framework of the intermediate-field theory[13–15] were found to agree very well with the parameters derived from a best-fit procedure on the basis of the high-field adiabatic theory.[3,6,7]

In this paper the energies *and* oscillator strengths of transverse excitons [σ spectra in Faraday ($\vec{k} \parallel \vec{H}$) and π spectra in Voigt ($\vec{k} \perp \vec{H}$) configuration] and of longitudinal-transverse mixed-mode excitons (σ spectra in Voigt configuration) as calculated by the intermediate-field theory are compared with the results of a *line-shape analysis* of exciton reflection spectra of InP and GaAs taken for Faraday and Voigt configuration in magnetic fields up to 20 T. The ratio of oscillator strengths of the pairs $\sigma^+_{\text{strong}}/\sigma^+_{\text{weak}}$, $\sigma^-_{\text{strong}}/\sigma^-_{\text{weak}}$, and $\pi_{\text{strong}}/\pi_{\text{weak}}$ is a function of the analytical exchange splitting Δ_a (Fig. 1).[14,16] The difference between the exciton energies and oscillator strengths for Faraday and Voigt configuration is mainly a function of the nonanalytical exchange-interaction (L-T—splitting constant) Δ_{LT}. Therefore we are able to derive simultaneously in a rather direct manner the size of both interactions. It is found that the analytical exchange splitting is extremely small, but definitely positive; whereas the L-T—splitting constant is of the order of $\approx \frac{1}{10}$ meV for both materials.

The paper is organized in the following way: In Sec. II we will discuss the various $\vec{k}$-dependent parts of the exciton Hamiltonian. The different types of exciton states in a magnetic field are explained by the competitive quantization due to different directions of the wave vector $\vec{k}$ and the magnetic field $\vec{H}$. In Sec. III we give a short phenomenological theory of magnetoexcitons and magnetopolaritons. A relation connecting the magnetopolariton states at $\vec{k}=\vec{0}$ in Faraday and Voigt configuration is derived. After that we discuss the model of an exponentially decreasing exciton-free layer to get a best fit of the experimental magnetoreflectivity line shape. Section IV is devoted to some experimental details. In Sec. V we give a detailed comparison between theory and experiment. Section VI is the conclusion.

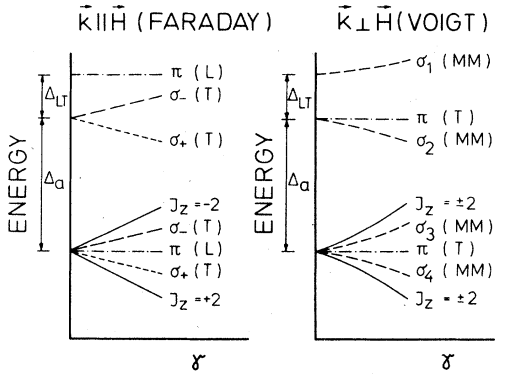

FIG. 1. Schematic splitting and polarization pattern of the $F=1$ (top) and $F=2$ (bottom) exciton states in a semiconductor with Γ_6 conduction and Γ_8 valence band in the presence of an external magnetic field. For Faraday configuration (wave vector $\vec{k}$ of the light parallel to the magnetic field direction $\vec{H}$) the eigenstates are purely longitudinally (L) and transversely (T) polarized with respect to $\vec{k}$. For Voigt configuration ($\vec{k} \perp \vec{H}$) all σ states are mixed modes (MM) and only the π states are purely transverse modes. The cubic anisotropy of the analytical part of the exchange is neglected for simplicity here. Δ_a is the analytical and Δ_{LT} the nonanalytical exchange splitting.

II. $\vec{k}$ DEPENDENCE OF THE EXCITON

The various $\vec{k}$-dependent terms of the Schrödinger equation, where $\vec{k}$ is a generalized momentum of the center of mass[17] of the exciton in a magnetic field, are briefly discussed in this section, and a $\vec{k}$-dependent classification of transverse, longitudinal, and mixed-mode excitons is given.

In an external magnetic field $\vec{H}$ all electromagnetic wave phenomena depend on the angle between $\vec{H}$ and the direction of propagation of the wave $\vec{k}$. The magnetic field introduces optical anisotropies even in the case of an "isotropic crystal." In a real crystal (e.g., a cubic one) the magnetic-field-induced anisotropies depend further on the direction of the field $\vec{H}$ relative to the crystal axis. Since the optical properties of an ideal semiconductor in the near band-gap region are governed by excitons, a microscopic theory of the field-induced anisotropies (e.g., Faraday and Voigt effect) in this frequency range has to result in $\vec{k}$-dependent exciton spectra, even in the case of an isotropic crystal. A cubic semiconductor like GaAs is an example for such a system if the cubic anisotropy of the valence band is neglected. The exciton Hamiltonian in a magnetic field includes three $\vec{k}$-dependent terms which result from the solution of the Schrödinger equation in the following way:

Separating the center-of-mass coordinate $\vec{R}$ by[15]

$$\Phi_{\text{ex}}(\vec{r}_e,\vec{r}_h) = \frac{1}{\sqrt{\Omega}} \exp\left[i\left(\vec{k}+\frac{e}{\hbar c}\vec{A}(\vec{r})\right)\cdot\vec{R}\right] \times \sum_{J_c J_v} F^{\vec{k}}_{J_c J_v}(\vec{r})\, U_{J_{c,0}}(\vec{r}_e)\, K U_{J_{v,0}}(\vec{r}_h) \quad , \tag{1}$$

the set of envelope functions $F^{\vec{k}}_{J_c J_v}(\vec{r})$ turns out to be a solution of the following set of equations:

$$\sum_{j_c' j_v'} \left[H_{j_c j_c'}\left(\vec{p}+\frac{e}{c}\vec{A}(\vec{r})+\frac{\alpha}{2}\hbar\vec{k}\right)\delta_{j_v j_v'} - H_{j_v' j_v}\left(-\vec{p}+\frac{e}{c}\vec{A}(\vec{r})+\frac{\beta}{2}\hbar\vec{k}\right)\delta_{j_c j_c'} - \frac{e^2}{\epsilon_0 r}\delta_{j_c j_c'}\delta_{j_v j_v'} + [I(\vec{k})]_{j_c j_v' j_c' j_v} \right] \times F^{\vec{k}}_{j_c' j_v'}(\vec{r}) = E_{ex}(\vec{k}) F^{\vec{k}}_{j_c j_v}(\vec{r}) \quad . \quad (2)$$

In Eqs. (1) and (2) we used the following notations: $\vec{r}_e, \vec{r}_h$ are the coordinates of the electron and hole; $\vec{r}=\vec{r}_e-\vec{r}_h$, $\vec{R}=\alpha\vec{r}_e+\beta\vec{r}_h$, $\alpha=m_e/(m_e+m_h)$, $\beta=1-\alpha$, and $m_h^{-1}=\gamma_1/m_0$, m_0 is free-electron mass, γ_1 is the Kohn-Luttinger parameter of the valence band; $\vec{p}$ is the linear momentum of the relative motion of the exciton; $\vec{A}$ is the vector potential of the external magnetic field; and $H_{j_c j_c'}, H_{j_v' j_v}$ are the Kohn–Luttinger-type matrices describing the bottom of the conduction bands j_c and the top of the valence bands j_v in the effective-mass approximation. $U_{j_{c,0}}, U_{j_{v,0}}$ are the Bloch factors at the bottom of the conduction band and the top of the valence band; K is the time-reversal operator; ϵ_0 is the static dielectric constant of the crystal; $\delta_{j_c j_c'}, \delta_{j_v j_v'}$ are the Kronecker symbols; I stands for electron-hole exchange interaction, and means a many-particle correction to an effective-mass description of the exciton. Only this type of many-particle correction is included since it mainly controls the splittings of an otherwise degenerate set of excitons as a solution of an effective-mass calculation.[15]

The three $\vec{k}$-dependent terms of Eq. (2) are quite different in their size and their physical meaning:

(a) The nonanalytical (long-range) part of the electron-hole exchange interaction is already present in the field-free case. It is the most important term depending on the *direction* of $\vec{k}$ and it does not vanish for $\vec{k}\to 0$.[15] Since this term represents a contact potential $\sim\delta(\vec{r})$ it is proportional to the excitonic oscillator strengths. Therefore a strong enhancement of this term is to be expected in a large magnetic field where the wave function starts to shrink.

(b) The kinetic energy $\hbar^2k^2/2M_{ex}$ of the exciton center of mass vanishes in the limit $\vec{k}\to 0$.[18,19] This term introduces the spatial dispersion in the optical properties of excitons.

(c) The $\vec{k}\times\vec{H}$ term contributes a field-dependent part to the dispersion relation of excitons or polaritons. It gives rise to a magneto-Stark effect. In crystals with *weakly* disturbed inversion symmetry (e.g., GaAs and InP) its influence on the excitonic-ground-state $1s$ multiplet might be small for small $\vec{k}$ values which are the only ones of relevance here. In contrast to this, the $\vec{k}\times\vec{H}$ term has some influence on the $2s$-$2p$ splitting (e.g., of the exciton in CdS).[20]

For small $\vec{k}$ values the nonanalytical electron-hole exchange interaction can be expected to be the most important $\vec{k}$-dependent contribution in the exciton Hamiltonian. The terms (b) and (c) are caused by the finite translational mass of the exciton. Term (a) has quite another origin: it represents the electrostatic interaction energy of the induced polarization charge $-\mathrm{div}\vec{P}_{ex}$ of the longitudinal part of the excitonic polarization with its own electric field.

This term depends on the excitonic oscillator strengths as mentioned above and has nothing to do with any translational mass effect! At zero magnetic field and for *small* cubic anisotropies longitudinal and transverse excitons are good eigenstates of the Hamiltonian independent of the direction of $\vec{k}$ (for $\vec{k}\to 0$). In an external magnetic field the terms longitudinal and transverse are meaningful only for Faraday configuration $\vec{k}\parallel\vec{H}$, since in general the magnetic field introduces another axis of quantization, which is competitive to the direction of $\vec{k}$ (see Fig. 1). In a general direction of $\vec{k}$ longitudinal and transverse excitonic states are coupled.[16] The general mode in the presence of a magnetic field is then a coupled "magnetoplasma"-photon mode,[21] a coupled state of a transverse photon field and a longitudinal-transverse mixed mode of the excitonic polarization field.

Three different types of exciton spectra in cubic crystals in a magnetic field are expected due to the nonanalytical exchange interaction. These are in order of increasing complexity (see Fig. 1):

(a) Faraday geometry, $\vec{k}\parallel\vec{H}$: There exist *pure* transverse (σ^+, σ^-) and longitudinal (π) exciton states. But in sharp contrast to the zero-field case, the tensor of the dielectric constant cannot be diagonalized by choosing a system of axes in *real space.* The tensor is diagonal only in the "polarization representation" $\sigma^+(x+iy)$, $\sigma^-(x-iy)$, and $\pi(z)$, where z is parallel to the field direction.

(b) Voigt geometry, $\vec{k}\perp\vec{H}$: Transverse (π) and longitudinal-transverse mixed-mode excitons (coupled σ^+, σ^- states) are formed. This case is similar to a general direction in an uniaxial crystal like CdS (with the exception of lacking time-reversal symmetry in the presence of a magnetic field).

(c) General geometry, $\vec{k}\cdot\vec{H}\neq 0, kH$: Only π, σ^+, σ^--coupled mixed modes are eigenstates of the Hamiltonian. This case resembles the situation in a biaxial crystal.

Since we compare theory and experiment for Faraday and Voigt configuration on the basis of the field-dependent solutions of Eq. (2) including the directional-dependent exchange interaction we give the two potentials for $\vec{k}\parallel[001]\parallel\vec{H}$ and $\vec{k}\parallel[100]\perp\vec{H}$

as follows (we consider only excitons being constructed from the Γ_6 conduction band and the Γ_8 valence band):

$$I(\vec{k}) = I_{\text{analytical}} + I_{\text{nonanalytical}}(\vec{k}) \ , \tag{3a}$$

$$I_{\text{analytical}} = \tfrac{1}{4}\Delta_a \pi a_0^3 \delta(\vec{r}) \begin{pmatrix} 3 & 0 & 0 & 0 & 0 & \sqrt{3} & 0 & 0 \\ & 2 & 0 & 0 & 0 & 0 & 2 & 0 \\ & & 1 & 0 & 0 & 0 & 0 & \sqrt{3} \\ & & & 0 & 0 & 0 & 0 & 0 \\ & & & & 0 & 0 & 0 & 0 \\ & & & & & 1 & 0 & 0 \\ & & & & & & 2 & 0 \\ & & & & & & & 3 \end{pmatrix} , \tag{3b}$$

$$I_{\text{nonanalytical}}(\vec{k} \parallel [001]) = \tfrac{1}{2}\Delta_{LT} \pi a_0^3 \delta(\vec{r}) \begin{pmatrix} 0 & 0 & 0 & 0 & 0 & 0 & 0 & 0 \\ & 1 & 0 & 0 & 0 & 0 & 1 & 0 \\ & & 0 & 0 & 0 & 0 & 0 & 0 \\ & & & 0 & 0 & 0 & 0 & 0 \\ & & & & 0 & 0 & 0 & 0 \\ & & & & & 0 & 0 & 0 \\ & & & & & & 1 & 0 \\ & & & & & & & 0 \end{pmatrix} , \tag{3c}$$

$$I_{\text{nonanalytical}}(\vec{k} \parallel [100]) = \tfrac{1}{8}\Delta_{LT} \pi a_0^3 \delta(\vec{r}) \begin{pmatrix} 3 & 0 & -\sqrt{3} & 0 & 0 & \sqrt{3} & 0 & -3 \\ & 0 & 0 & 0 & 0 & 0 & 0 & 0 \\ & & 1 & 0 & 0 & -1 & 0 & \sqrt{3} \\ & & & 0 & 0 & 0 & 0 & 0 \\ & & & & 0 & 0 & 0 & 0 \\ & & & & & 1 & 0 & -\sqrt{3} \\ & & & & & & 0 & 0 \\ & & & & & & & 3 \end{pmatrix} . \tag{3d}$$

In Eqs. (3b)–(3d) we used the following notations: $a_0 = \hbar^2 \epsilon_0 / \mu_0 e^2$ with $\mu_0^{-1} = m_e^{-1} + \gamma_1 / m_0$, $\delta(\vec{r})$ is the Dirac δ function, Δ_0 is the isotropic part of the zero-field analytical part of the exchange interaction, and Δ_{LT} is the zero-field L-T splitting of the dipole-allowed Γ_5 exciton.

III. PHENOMENOLOGICAL DIELECTRIC THEORY

Reflection experiments give information on excitons because the dielectric constant and therefore the index of refraction are modulated by the presence of exciton states with finite dipole moments. In this section a short description of magnetoexcitons in terms of Maxwell's equations is given and the quantum-mechanical description is linked to the dielectric theory.

The dispersion relations for normal waves[22] in dielectrics are given as the roots of the following general equation:

$$\det\left[\frac{\omega^2}{c^2}\epsilon_{ij}(\vec{k}, \omega, \vec{H}) - k^2\delta_{ij} + k_i k_j\right] = 0 \ , \tag{4}$$

where ω is the frequency, c is the velocity of light in vacuum, $\vec{k}$ is the wave vector of the normal mode being excited, and ϵ_{ij} is the i,j component of the dielectric tensor, $i,j = x,y,z,$. $\vec{H}$ is the external magnetic field not to be confused with the weak magnetic field of the normal wave.

The principle of symmetry of the kinetic coefficients[22,23] yields the general symmetry relation

$$\epsilon_{ij}(\vec{k}, \omega, \vec{H}) = \epsilon_{ji}(-\vec{k}, \omega, -\vec{H}) \ . \tag{5}$$

If the dielectric is assumed to be free of loss the dielectric tensor ϵ_{ij} has to be a Hermitian tensor[22,24]

$$\epsilon_{ij}(\vec{k}, \omega, \vec{H}) = \epsilon_{ji}^*(\vec{k}, \omega, \vec{H}) \ . \tag{6}$$

This ϵ is then completely determined (besides a "background" part ϵ_b) by the solutions of Eq. (2), being the basis of a microscopic theory.

Assuming the external magnetic field to be in z direction (parallel to the [001] axis of the cubic crystal) from Eq. (4) a relation between ω and $\vec{k}$ can be derived[25]

$$\tan^2(\theta) = -\frac{[1 - (c^2k^2/\omega^2\epsilon_+)][1 - (c^2k^2/\omega^2\epsilon_-)]}{[1 - (c^2k^2/\omega^2\epsilon_{zz})][1 - (c^2k^2/\omega^2\epsilon')]} \ . \tag{7}$$

In Eq. (7) the following abbreviations were used:

$$\epsilon_{\pm} \equiv \epsilon_{\pm}(\vec{k}, \omega, \vec{H}) = \epsilon_{xx} \pm i\epsilon_{xy} \ , \tag{8a}$$

$$\epsilon' \equiv \epsilon'(\vec{k}, \omega, \vec{H}) = \frac{\epsilon_+ \epsilon_-}{\frac{1}{2}(\epsilon_+ + \epsilon_-)} \tag{8b}$$

and θ is the angle between $\vec{k}$ and $\vec{H}$. If we now concentrate on the configurations $\vec{k} \parallel \vec{H}$ and $\vec{k} \perp \vec{H}$, we immediately obtain the dispersion relations:

(a) Faraday geometry, $\theta = 0$

$$\frac{c^2k^2}{\omega_+^2} = \epsilon_+ \ , \quad \frac{c^2k^2}{\omega_-^2} = \epsilon_- \ , \quad \epsilon_{zz} = 0 \ . \tag{9}$$

The first two solutions of Eq. (9) yield left and right circular-polarized transverse polariton states and the third solution represents a longitudinal exciton.

(b) Voigt geometry, $\theta = \frac{1}{2}\pi$

$$\frac{c^2k^2}{\omega_z^2} = \epsilon_{zz} \ , \quad \frac{c^2k^2}{\omega'^2} = \epsilon' \ . \tag{10}$$

The first solution of Eq. (10) is a transverse linearly polarized polariton state and the second characterizes longitudinal-transverse mixed-mode polaritons. Let us discuss these mixed modes first without coupling them to photons. Then we have to look for the singularities of ϵ' or, from Eq. (8b), the zeros of

$$\tfrac{1}{2}(\epsilon_+ + \epsilon_-) = \epsilon_{xx} = 0 \ . \tag{11}$$

We have in this case a coupled mode between transverse excitonic polarization, longitudinal excitonic polarization, and longitudinal electric field. Due to its mixed-mode character this normal wave can be excited by transverse perturbations as well as by longitudinal ones. Therefore from the second of the Eqs. (10) the square of the index of refraction for *light* being polarized in a plane perpendicular to the magnetic field $\vec{H}$ can be calculated and yields coupled states of transverse and longitudinal polarization and transverse and longitudinal electric fields!

Due to the different coupling schemes in both geometries we obtain different states and frequencies for σ-polarized states. However, there is one important exception. If we put $\vec{k} = 0$ in the equations above, it is easily seen with the help of Eq. (8b) that the polariton energies at $\vec{k} = 0$ for σ-polarized states agree in both geometries. The zeros of $\epsilon'(0, \omega, \vec{H})$ agree with those of $\epsilon_+(0, \omega, \vec{H})$ *and* $\epsilon_-(0, \omega, \vec{H})$. This relation has been used as a check for all numerical computations for both geometries.

So far we have only discussed the relation between the zeros of the dielectric constant and the solution of the Schrödinger equation in intermediate magnetic fields. If we want to compare theory and experiment we have to go one step further and include the effect of a surface layer of the crystal, where the exciton does not contribute to the dielectric function of the crystal. This so-called "dead layer" or "exciton-free layer" strongly alters the actually measured reflectivity of a crystal. In a first approximation the reflection of an electromagnetic wave on the surface of a semiconductor can be described in a three-layer model [see Fig. 2(a)] with: (i) Vacuum with refraction index $n_1 = 1$. (ii) Dead layer with refraction index $n_2 = (\epsilon_b)^{1/2}$, where ϵ_b is the background dielectric constant. The surface acts as a potential repelling the excitons within a certain depth. This depth depends on the exciton diameter. (iii) Inside the crystal the exciton contributes to the dielectric properties. The index of refraction is frequency- and momentum-dependent, as discussed above, and approximately given by

$$n_3 = \frac{ck}{\omega} = \left(\epsilon_b + \frac{4\pi\alpha_0\omega_T^2}{\omega_T^2 + \omega_T \hbar k^2/M - \omega^2 - i\omega\Gamma_b} \right)^{1/2} \ . \tag{12}$$

Here $4\pi\alpha_0$ is the oscillator strength, ω_T is a solution of the exciton Schrödinger equation for a certain configuration and Γ_b is the damping constant of the bulk. M is the total mass of the exciton. The k dependence of the latter one[26] is neglected here. If the exciton is simply excluded from a surface layer of thickness l, then the reflectance R is a function of two interfering waves with phase difference ϕ. R is then given by

$$R = \left| \frac{n^* - 1}{n^* + 1} \right|^2 \ , \tag{13}$$

where n^* is a function of the phase angle $\theta = 2qn_2l$ and of the different indexes of refraction as discussed in Ref. 3. A change of the thickness l of the exciton-free layer and therefore a change of the phase lag between the two interfering waves completely changes the line shape. This effect was recently used to measure for the first time directly the anisotropy of the exciton wave function in a magnetic field.[27]

However, a rectangular exciton-free layer with an abrupt change of the damping from infinite inside to a very low level value at the end of the layer is only a crude approximation. This model was recently[28] much refined by introducing an exponentially decreasing damping within the depth Q [see Fig. 2(b)]. The reflectance then has to be calculated by means of a multiple reflection model, approximating the exponential function $\Gamma \sim e^{-x/a}$ by a step function. A much improved fit to the experimental data resulted. Figure 3 gives as example GaAs at six different magnetic fields. In this figure the best fits of exciton reflection spectra in various magnetic fields are compared for a three-layer model and an exponential model. The difference is striking, and all experimental results were evaluated using the exponential model.

None of the experiments (except at zero magnetic field) shows only one single well-separated oscillator.

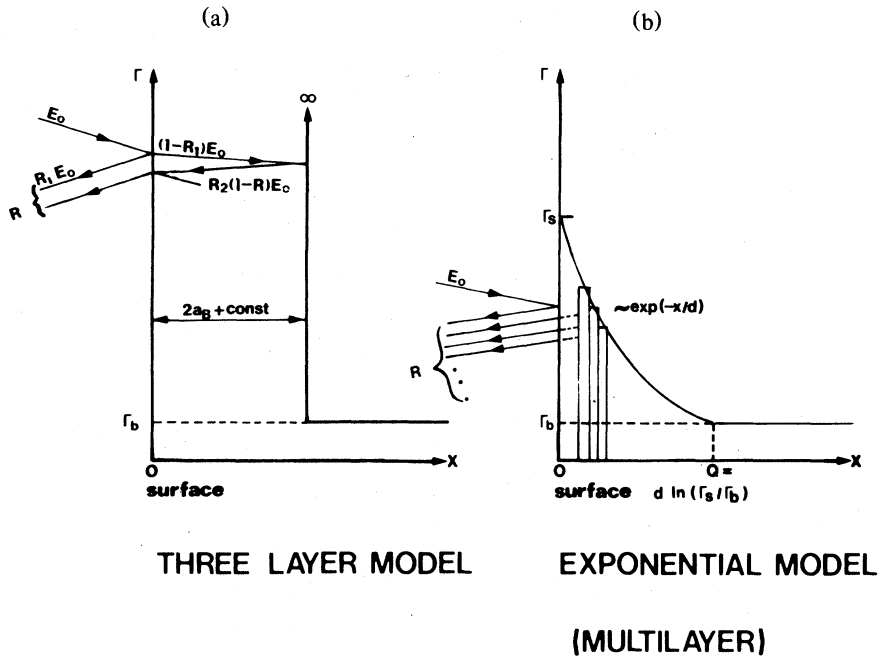

FIG. 2. Schematic picture of the reflectivity of a semiconductor (a) with a square-well exciton-free layer (infinite damping); (b) with an exponentially decreasing damping of the exciton contribution on the surface. (Γ_b, Γ_s: damping levels in the interior of the crystal and at the surface; R, R_1, R_2: reflectivities of the half space and of the various interfaces; E_0: incident intensity; $2a_B$: diameter of the exciton.)

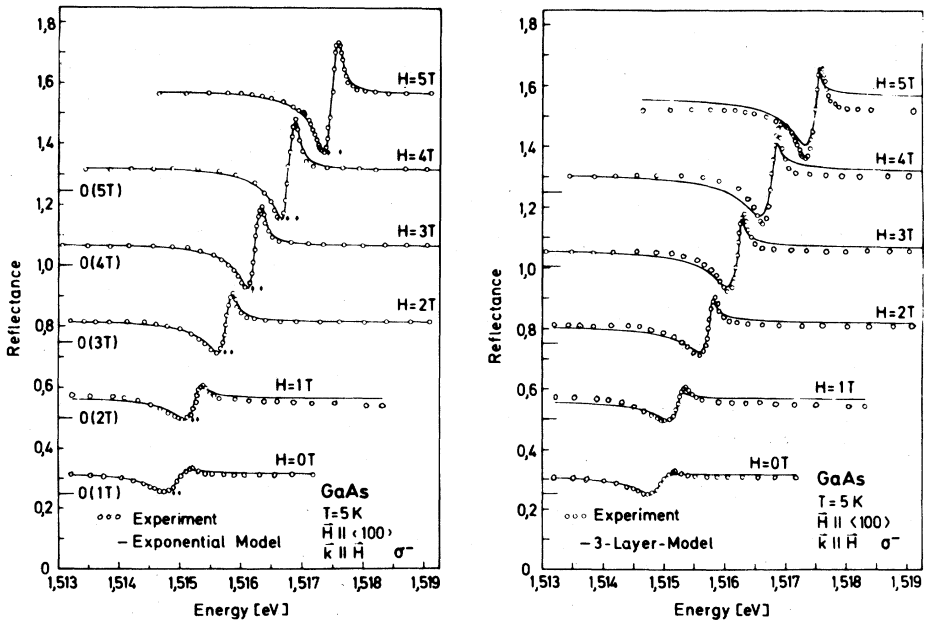

FIG. 3. Comparison of σ^--polarized spectra (open circles) with a theoretical line-shape fit using a three-layer model (right) and an exponential model for the exciton-free layer (left) on the surface of the crystal. In both cases a least-mean-square fit with two coupled oscillators was employed. Although the number of fitting parameters is the same for both models, the exponential model yields a much improved fit, particularly at higher fields. The position of the longitudinal and transverse exciton states is given by arrows. Note the increase of the L-T splitting with increasing field. For clarity the different reflection curves are displayed vertically against each other and the different baselines are given by a dash on the vertical scale.

The oscillators always appear as doublets (σ^+, σ^-, π) or as a quartet (σ in Voigt) in a magnetic field. The interaction between the oscillators was taken into account by using a two-oscillator model for the evaluation of the data as discussed in detail in Ref. 29. This procedure is, of course, only an approximation in the four-oscillator case.

Experimental values of the field dependence of the polariton energies and oscillator strengths—as far as they are relevant for the calculation of the constants Δ_a and Δ_{LT} of the exchange interaction—derived from the spectra in the way discussed above, are presented in Sec. V. A short account of the experimental procedure is given in Sec. IV.

IV. EXPERIMENTAL

All reflection experiments were done with predispersed light of a bandwidth $\Delta\lambda \approx 0.1$ Å, employing light levels as low as possible to avoid heating and free-carrier effects. In contrast to earlier experiments, a weak He-Ne laser of some μW power excited the part of the sample from which the light was reflected. In this way free carriers were created to assure flat band conditions.[8] The angle of incidence of the test light was 4° in all experiments. An achromatic Fresnel rhomb, together with a Polaroid linear polarizer, was used to polarize the light. All crystals used were of very high purity. They were grown by E. Bauser (Max-Planck-Institut für Festkörperforschung, Stuttgart), K. Fairharst (Royal Signals and Radar Establishment, Gt. Malvern), and P. Rosetto (Kristallabor, University of Stuttgart). Typical impurity concentrations and mobilities were $N_D - N_A = 8 \times 10^{13}/\text{cm}^3$, $\mu = 170\,000$ cm^2/V sec for GaAs, and $N_D - N_A = 2 \times 10^{14}/\text{cm}^3$, $\mu = 100\,000$ cm^2/V sec for InP. More experimental details are given in Refs. 3 and 29.

V. RESULTS AND DISCUSSION

In this section first experimental and theoretical results for the σ^-, σ^+ levels in Faraday geometry and the π levels in Voigt geometry are compared with each other for GaAs and InP. An upper limit for the isotropic part of the analytical exchange interaction is derived for both materials from this comparison.[30] Then the nonanalytical exchange constant Δ_{LT} is determined from the mixed-mode spectra.

A. Determination of the analytical exchange constant Δ_a

(i) InP. In Figs. 4(a)–4(c) the results of a best fit of the theory to the experimental σ^+, σ^-, and π exciton energies are shown. The input parameters for

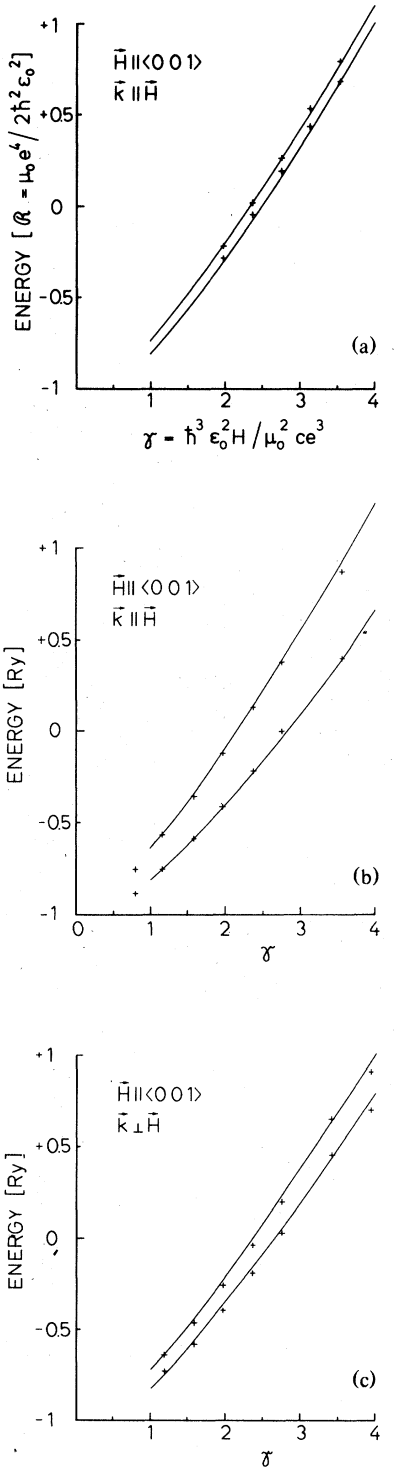

FIG. 4. Comparison of experimental values (crosses) of transverse exciton energies in InP determined from a lineshape fit as a function of a magnetic field with theoretical values for (a) σ^+ polarization, (b) σ^- polarization, and (c) π polarization. The input parameters used for the calculation are given in the text.

these fits are

$\gamma_1 = 4.95$, $\gamma_2 = 1.85$, $\gamma_3 = 2.55$, $k = 0.97$,

$q = 0.0$, $m_e = 0.0803 m_0$, $g_e = 1.31$.

They agree very well with the values derived from a fit to the adiabatic high-field theory.[7] As can be seen from Fig. 4, theory and experiment are in good agreement with each other. Experimentally determined *transverse* exciton levels are compared with the theoretical results here and not only the minima of the reflection curves. Therefore no assumptions concerning the zero-field L-T splitting had to be made. Since the energies do not depend strongly on Δ_a and Δ_a is expected to be rather small, the energy comparison provides the input data for the calculation of the oscillator strengths. On the other hand, the value of Δ_a deterimes in a very sensitive manner the ratio of the oscillator strenths of the three doublets. Figure 5(a) gives an excellent example for the σ^+ pair in InP. We start at $\Delta_a = 0$ with a strong lower line and a weak upper one and arrive then at a value of $\Delta_a = 0.04$ (measured in units of the zero-field excitonic Rydberg $R = \mu_0 e^4 / 2\hbar^2 \epsilon_0^2$) at a strong upper line and weak lower one. Figure 5(b) shows the theoretical oscillator strengths for the π case at different values of Δ_a. For $\Delta_a = 0$ the ratio of the oscillator strengths of the two π components is very close to 1, as expected from atomic theory. At larger values of Δ_a we obtain a strong upper level and a weak lower one. In Fig. 5(c) the experimentally determined ratio and sum of the oscillator strengths for the π polarized lines are compared with the results of the present theory. Our result for the sum of the oscillator strengths agrees very well with the oscillator strengths of an exact numerical calculation of an isotropic spinless hydrogenic problem by Cabib *et al.*[31] The ratio of the oscillator strengths yields an extremely small value of Δ_a of $\sim(0.0075 \pm 0.003) R$. These values agree quite well with theoretical estimates from band-structure calculations.[32] As to the sum of the oscillator strengths, the agreement between theory and experiment is also very good. In this connection it should be stressed that theoretical oscillator strengths are much more sensitive on the approximation chosen for the solution of the eigenvalue problem than the energies. This is best demonstrated by the Table II of Ref. 13 where the adiabatic oscillator strengths measured in zero-field units are compared with the oscillator strengths of Cabib *et al.*[31] A large discrepancy of the two sets of oscillator strengths is found there in contrast to the good agreement found here. The results obtained from the comparison of experiment with theory for the σ^-, σ^+ components agree with this result and are therefore not further discussed.

(ii) GaAs. Figures 6(a)–6(c) give a comparison between experimental transverse exciton energies and

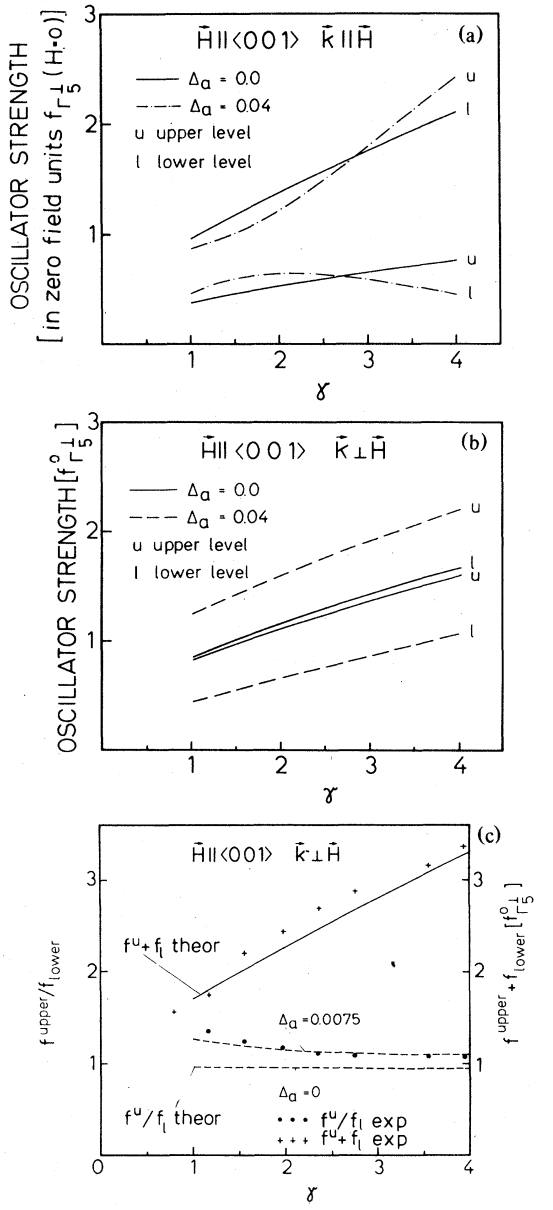

FIG. 5. Theoretical magnetic field dependence of the oscillator strengths of the two transversely σ^+ (a) and π (b) polarized oscillators in InP for two different values Δ_a of the analytical part of the exchange interaction. In (c) the experimental and the theoretical field dependence of the ratio (left scale) and of the sum (right scale) of the oscillator strength of the two π oscillators are compared with each other for two values of Δ_a.

the best fit of the theory for the σ^+, σ^-, and π spectra of GaAs. The agreement between theory and experiment is as good as in the case of InP. The input parameters are

$\gamma_1 = 7.05$, $\gamma_2 = 2.35$, $\gamma_3 = 3.0$, $k = 1.28$,

$q = 0.04$, $g_c = 0.46$, $m_e = 0.0665 m_0$.

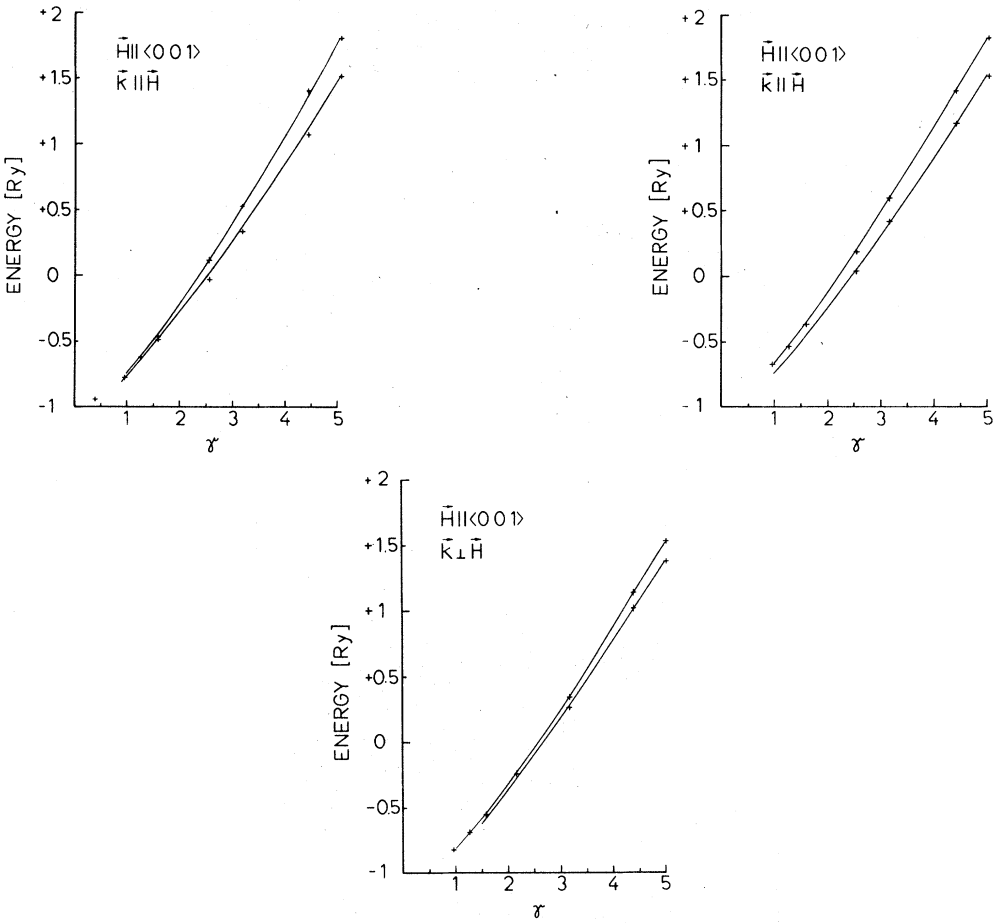

FIG. 6. Comparison of experimental values (crosses) of transverse exciton energies in GaAs determined from a line-shape fit as a function of a magnetic field with theoretical values for (a) σ^+ polarization, (b) σ^- polarization , and (c) π polarization. The input parameters used for the calculation are given in the text.

In Fig. 7 the experimental oscillator strengths $f^{\text{upper}}/f_{\text{lower}}$ are compared with the theoretical ones for the π spectra. From the variation of $f^{\text{upper}}/f_{\text{lower}}$ as a function of Δ_a a value of $\Delta_a \sim (0.005 \pm 0.002)R$ is derived. Since the band structures and effective masses of GaAs and InP are rather similar, similar values of Δ_a for both materials are not astonishing. The value of $\Delta_a = 0.02 \pm 0.008$ meV for GaAs roughly agrees with Sell's value[33] of $\Delta_a = 0.1 \pm 0.1$ meV which was obtained from piezoreflection measurements and is in direct contrast to the value 0.37 meV obtained previously by Gilleo *et al.*[34] from stressed luminescence studies and to the value 0.38 meV obtained by Abe[35] from a variational calculation. It is believed, however, that the value of Δ_a being derived here is more convincing since it is derived from the ratio of the oscillator strengths, which is much more sensitive to a small variation of Δ_a than the energetic splittings. Although Δ_a is rather small for both materials, it is clearly positive, larger than zero!

B. σ mixed modes (Voigt geometry)

The numerical calculations of mixed-mode energies and oscillator strengths are performed in the following way: We start from the set of functions Eqs. (28a) and (28b) of Ref. 15, which were first used separately to calculate the σ^+ and σ^- states in Faraday geometry. Then the nonanalytical part of the electron-hole exchange interaction is taken into account. Two new effects result. First we get a separate *intra-series* coupling of the σ^+ and σ^- states, an effect that has been discussed in detail in Ref. 14. This coupling results simply in a replacement of the constant Δ_a by $\Delta_a + 0.5\Delta_{LT}$. Second, σ^+ and σ^- states are coupled by the inter-series matrix elements of the LT-splitting potential. This coupling causes that only mixed modes are solutions of the exciton Hamiltonian. The transverse dielectric constant ϵ' and its zeros are then calculated using the mixed-mode energies and oscillator strengths. As described

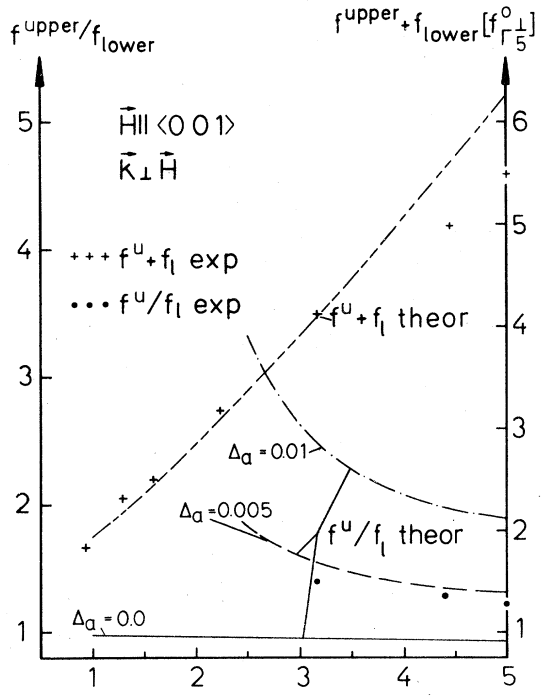

FIG. 7. Comparison of the experimental field dependence of the ratio (circles) and the sum (crosses) of the oscillator strength of the two π oscillators in GaAs with theoretical predictions for three different values of the analytical exchange interaction Δ_a.

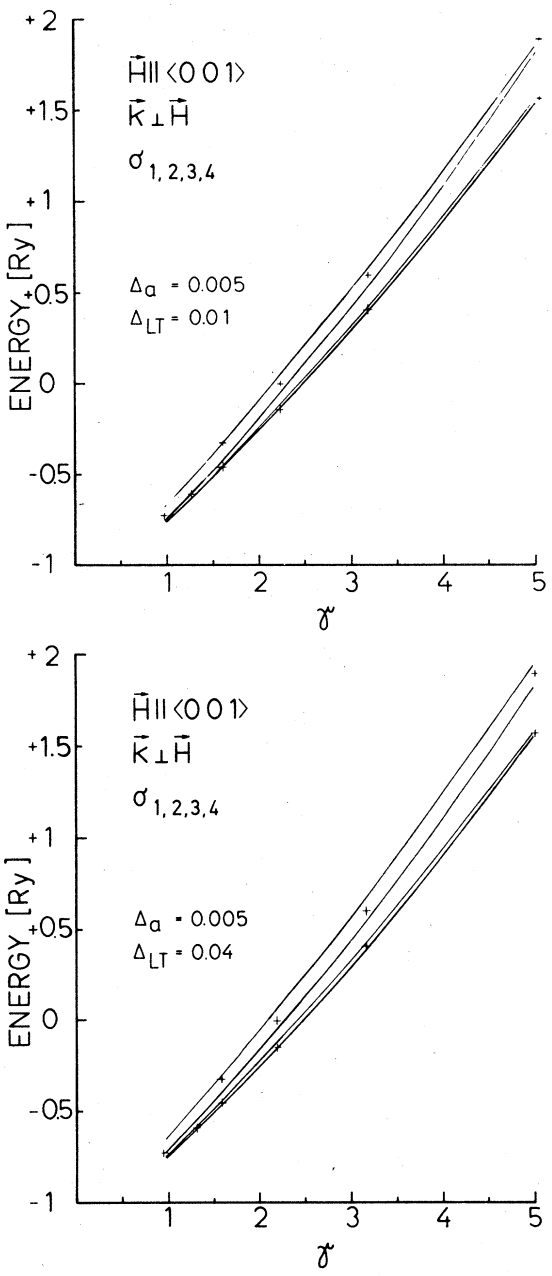

FIG. 8. Comparison of the theoretical magnetic field dependence of the four mixed modes in Voigt geometry with the experimentally determined energies of the two strongest components of the quartet for two different values of $\Delta_{LT}=0.01$ and 0.04 R and the same $\Delta_a=0.005$ R in GaAs.

in Sec. III, they have to agree with those calculated from ϵ_+ and ϵ_- for $\vec{k}=0$. This is indeed the case within the numerical accuracy.

In the framework of the theory used here, there is just *one* new parameter, the zero-field LT-splitting constant Δ_{LT}, which has to account for all differences at the same time found between the Faraday and Voigt spectra. Therefore it is thought that this comparison of the σ-polarized exciton spectra for Voigt and Faraday geometry establishes an accurate value for the zero-field LT-splitting constant Δ_{LT}.

In Figs. 8(a) and 8(b) we present theoretical mixed-mode energies for GaAs as a function of Δ_{LT}. They are compared to the experimental values taken from a line-shape analysis of the two strongest components of the quartet giving the most reliable results. It is obvious that by changing Δ_{LT} by a factor of 4 the quality of the fit is merely changed, indicating again the insensitivity of the exciton energies to the very small exchange energies. Therefore again the oscillator strengths which are much more sensitive and their dependence on the magnetic field are evaluated. Figure 9 compares the theoretical ratio of the oscillator strengths of the two lower to the two higher oscillators for five different values of Δ_{LT} with some experimental results. A value of $\Delta_{LT}\approx(0.02\pm0.01)\times R\,(\cong 0.08\pm0.04$ meV) is derived. This value disagrees somewhat with Sell's value[32] of $\Delta_{LT}=0.1-0.25$ meV. However, it agrees perfectly with recent results obtained from Brillouin scattering.[36]

For InP a line-shape analysis of the mixed modes

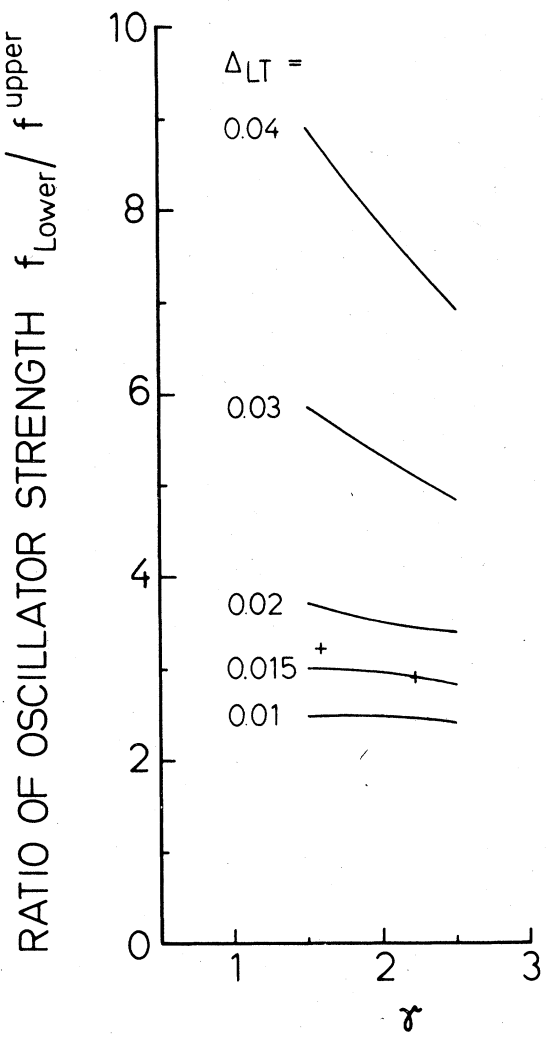

FIG. 9. Ratio of the oscillator strengths of the two energetically lower to the two energetically higher mixed modes of Fig. 8 for five different values of Δ_{LT} as a function of the magnetic field. Some experimental results are given by the crosses.

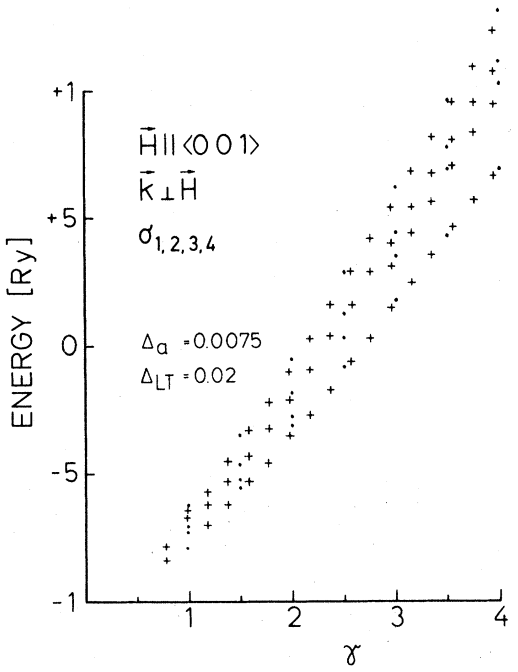

FIG. 10. Comparison of the zeros of the transverse dielectric constant (circles) with the experimentally determined minima of the reflectivity (crosses) as a function of the magnetic field in InP.

was hampered by computational difficulties. Therefore, we give only a fan chart (Fig. 10) showing the experimentally determined minima of reflectivity in comparison with the zeros of the transverse dielectric constant ϵ' for $\Delta_a = 0.0075R$ and $\Delta_{LT} = 0.02R$. From this we obtain as a rather crude upper boundary for $\Delta_{LT} \approx 0.1$ meV. But an exact value can be obtained, of course, only by a line-shape analysis. No other experimental or theoretical value for Δ_{LT} of InP is available for comparison, to the best of our knowledge.[37] Due to the similarity of the band structure, however, one would again expect a similar or slightly larger value as determined by us for GaAs in agreement with the above estimate.

VI. CONCLUSION

The magnetic field dependence of the energies and oscillator strengths of the 3×2 transverse exciton states σ^+, σ^-, and π in GaAs and in InP are calculated within the framework of an intermediate-field theory. Input parameters are the Luttinger parameters γ_1, γ_2, γ_3, κ, g, m_e, g_e, and the analytical exchange constant Δ_a. Since the energies depend only very weakly on the choice of Δ_a as far as it is reasonably small, a best fit to experimentally determined energies yields the Luttinger parameters which are found to be in good agreement with the values derived recently from a fit to an adiabatic high-field theory. The transverse exciton energies are identical with the poles of a dielectric function in the appropriate energy range. The poles are experimentally determined from a line-shape analysis of recent magnetoreflection experiments using a newly developed exponential model for the exciton-free layer on the surface of a semiconductor.

In contrast, the oscillator strengths are found to react most sensitively to the slightest variation of the exchange constant Δ_a. Thus this constant can be determined from a comparison with the experiments, with much higher precision than hitherto, to be $\Delta_a = 0.02 \pm 0.008$ meV for GaAs. For the first time a value for Inp $\Delta_a = 0.04 \pm 0.015$ meV is derived in the

same way.

The σ-polarized exciton eigenstates in Voigt configuration ($\vec{k} \perp \vec{H}$) are mixed longitudinal-transverse modes. The differences of their energies and oscillator strengths from those of the purely transverse σ^+, σ^- modes observed in Faraday configuration ($\vec{k} \parallel \vec{H}$) are a function of the nonanalytical part of the exchange interaction (L-T splitting) Δ_{LT}. Again model calculations within the framework of the intermediate-field theory show the dramatic dependence of the oscillator strengths of the mixed modes and their ratios to the actual value of Δ_{LT} in contrast to the energies, which are rather insensitive to it. From a comparison to experiment Δ_{LT} of GaAs is determined to 0.08 ± 0.02 meV, thus substantially supporting conclusions recently drawn from Brillouin experiments and revising somewhat a value derived from piezoreflection. An upper limit of $\Delta_{LT} = 0.1$ meV is given for InP in good agreement with expectation from a comparison of the two materials based on their similar band structure.

ACKNOWLEDGMENTS

The work of two of us (W. E. and K. L.) was supported generously by the Deutsche Forschungsgemeinschaft. Thanks are due to K. Hess for his initial participation in the experiments and to E. O. Kane for some stimulating discussions. We are very much indebted to K. Dransfeld, G. Landwehr, M. H. Pilkuhn, and H. J. Queisser for their continuing interest and support. It is a pleasure to thank H. Krath for his kind assistance with the experiments.

---

*Present address: Standard Elektronik Lorenz AG, Hellmuth-Hirth Str. 40, D-7000 Stuttgart 40.

†Present address: Institut für Halbleitertechnik der RWTH, Sommerfeld-Str., D-5100 Aachen.

[1]A. Baldereschi and N. O. Lipari, Phys. Rev. Lett. 25, 373 (1970); Phys. Rev. B 3, 439 (1971).

[2]For an excellent review of older work until 1962 see R. S. Knox, in *Solid State Physics, Suppl. 5,* edited by H. Ehrenreich, F. Seitz, and G. Turnbull (Academic, New York, 1963).

[3]D. Bimberg, in *Advances in Solid State Physics XVII,* edited by J. Treusch (Vieweg, Braunschweig, 1977), p. 195.

[4]W. Staude, Phys. Status Solidi B 43, 367 (1971).

[5]F. Evangelisti, J. U. Fischbach, and A. Frova, Phys. Rev. B 9, 1516 (1974).

[6]K. Hess, D. Bimberg, N. O. Lipari, J. U. Fischbach, and M. Altarelli, in *Proceedings of the 13th International Conference on Physics of Semiconductors,* edited by G. Fumi (Tipografia Marves, Rome, 1976), p. 142.

[7]D. Bimberg, K. Hess, N. O. Lipari, J. U. Fischbach, and M. Altarelli, Physica (Utrecht) B 81, 139 (1977).

[8]F. Evangelisti, A. Frova, and F. Patella, Phys. Rev. B 10, 4253 (1974).

[9]K. Cho, Phys. Rev. B 14, 4463 (1976).

[10]L. Swierkowski, Phys. Rev. B 10, 3311 (1974); Nuovo Cimento B 29, 340 (1975).

[11]M. Altarelli and N. O. Lipari, Phys. Rev. B 9, 1733 (1974); see also G. J. Rees, J. Phys. C 5, 549 (1972).

[12]A. Baldereschi (private communication).

[13]W. Ekardt, Solid State Commun. 16, 233 (1975).

[14]W. Ekardt, Solid State Commun. 22, 531 (1977).

[15]W. Ekardt, Phys. Status Solidi B 84, 293 (1977).

[16]M. Suffczynski, L. Swierkowski, and W. Wardzynski, J. Phys. C 8, L52 (1975); M. Suffczynski, J. Phys. C 8, L400 (1975); M. Suffczynski and L. Swierkowski, Optics Commun. 17, 184 (1976). Our Δ_a is equal to $2\Delta_1 - \frac{1}{3}\Delta_{1\ell}$ in the nomenclature of the above authors.

[17]L. P. Gorkov and I. E. Dzyaloshinski, Sov. Phys. JETP 26, 449 (1968).

[18]E. O. Kane, Phys. Rev. B 11, 3850 (1975).

[19]M. Altarelli and N. O. Lipari, Phys. Rev. B 15, 4898 (1977).

[20]D. G. Thomas and J. J. Hopfield, Phys. Rev. Lett. 5, 505 (1960); Phys. Rev. 124, 657 (1961).

[21]H. Kawimura, in *Polaritons,* edited by E. Burstein and F. De Martini (Pergamon, New York, 1974), p. 247.

[22]V. M. Agranovich and V. L. Ginzburg, *Spatial Dispersion in Crystal Optics and the Theory of Excitons* (Wiley, New York, 1966).

[23]L. D. Landau and E. M. Lifschitz, *Lehrbuch der Theoretischen Physik* (Akademie, Berlin, 1966), Vol. 5.

[24]L. D. Landau and E. M. Lifschitz, *Lehrbuch der Theoretischen Physik* (Akademie, Berlin, 1966), Vol. 8.

[25]E. Astrøm, Ark. Fys. 2, 443 (1950).

[26]E. O. Kane, Phys. Rev. B 11, 3850 (1975).

[27]J. U. Fischbach, W. Rühle, D. Bimberg, and E. Bauser, Solid State Commun. 18, 1255 (1976).

[28]K. Lösch and D. Bimberg, Verh. Dtsch. Phys. Ges. 12, 46 (1977); and unpublished.

[29]D. Bimberg and K. Lösch (unpublished) give a complete survey of the experimental results.

[30]The anisotropic part of the analytical exchange interaction was shown to be one order of magnitude smaller than the isotropic part; see W. Ekardt, Phys. Status Solidi B 68, 53 (1975).

[31]D. Cabib, E. Fabri, and G. Fiorio, Nuovo Cimento B 10, 185 (1972).

[32]E. O. Kane (private communication).

[33]D. D. Sell, S. E. Stokowski, R. Dingle, and J. V. Dilorenzo, Phys. Rev. B 7, 4568 (1975).

[34]M. A. Gilleo, P. T. Bailey, and D. E. Hill, J. Lumin. 112, 562 (1970).

[35]Y. Abe, J. Phys. Soc. Jpn. 19, 818 (1964).

[36]C. Weisbuch and R. G. Ulbrich, Phys. Rev. Lett. 39, 654 (1977).

[37]The values given by one of us, W. Ekardt, Solid State Commun. 15, 889 (1974), were derived using a rather crude and apparently invalid approximation to the detailed theory given in this paper.